Broadband Instantaneous Multi-Frequency Measurement Based on a Fourier Domain Mode-Locked Laser

Beibei Zhu[ID], Jian Tang, Weifeng Zhang, *Member, IEEE*, Shilong Pan[ID], *Senior Member, IEEE*, and Jianping Yao[ID], *Fellow, IEEE*

Abstract— **Broadband instantaneous multi-frequency measurement based on frequency-to-time mapping using a Fourier domain mode-locked (FDML) laser source is proposed and experimentally demonstrated. An electrically controlled silicon microdisk resonator (MDR) with an ultra-narrow linewidth of 60 pm (∼7.5 GHz) functioning as a fast tunable optical filter is used to implement the FDML to generate a linearly chirped optical waveform (LCOW) with a wide frequency-sweeping range of 0.5 nm. The LCOW is then mixed at a modulator with a microwave signal with its frequency to be measured, detected at a low-speed photodetector (PD) and sent to a narrow bandpass filter (BPF). When the difference between the instantaneous frequency of the LCOW and that of the signal to be measured is equal to the center frequency of the BPF, a short-duration temporal signal is produced, and the time location of the temporal signal represents the frequency of the signal to be measured. A proof-of-concept experiment is carried out. Both single and multi-tone microwave frequency measurements are experimentally demonstrated. The measurement range is as large as 20 GHz with a measurement resolution of 200 MHz and an accuracy better than ±100 MHz. The proposed method showcases a new method for instantaneous frequency measurement (IFM) with high performance in terms of multi-frequency identification, real-time measurement, and high measurement speed compared with traditional approaches, which is attractive for applications in modern radar, electronic warfare, communication, and cognitive radio systems.**

Index Terms— **Fourier domain mode locking (FDML), instantaneous frequency measurement (IFM), microwave photonics, silicon photonics, single-sideband (SSB) modulation.**

Beibei Zhu is with the Microwave Photonics Research Laboratory, School of Electrical Engineering and Computer Science, University of Ottawa, Ottawa, ON K1N 6N5, Canada, and also with the College of Electronic and Information Engineering, Nanjing University of Aeronautics and Astronautics, Nanjing 210016, China.

Jian Tang, Weifeng Zhang, and Jianping Yao are with the Microwave Photonics Research Laboratory, School of Electrical Engineering and Computer Science, University of Ottawa, Ottawa, ON K1N 6N5, Canada (e-mail: jpyao@uottawa.ca).

Shilong Pan is with the College of Electronic and Information Engineering, Nanjing University of Aeronautics and Astronautics, Nanjing 210016, China.

I. INTRODUCTION

INSTANTANEOUS frequency measurement (IFM) of a microwave or millimeter-wave signal is one of the most important measurement tasks in radar, electronic warfare, communications, and cognitive radio systems [1], [2]. With the rapid growth of modern electronic applications, requirements for large measurement range, multi-frequency measurement, large dynamic range, high resolution, high sensitivity, and low cost come to the fore. Currently, electronics-based techniques have widely been employed for IFM which are generally realized using electrical delay-lines, digital IFM, and electrical filters [3]. These techniques can achieve very high resolution but suffer mainly from relatively narrow operation bandwidth, high power consumption, and vulnerability to electromagnetic interference (EMI). Recently, photonic-assisted techniques for IFM to take advantage of ultra-fast measurement speed, broad bandwidth, low loss, and immunity to EMI have been investigated [4]–[6]. Generally, photonic-assisted IFM techniques can be divided into three categories: frequency-to-power mapping [7]–[20], frequency-to-space mapping [21]–[24], and frequency-to-time mapping [25]–[30].

For the techniques based on frequency-to-power mapping [7]–[20], a monotonic relationship between the frequency of a signal under test (SUT) and the ratio of two optical or microwave powers, defined as amplitude comparison function (ACF), is established. By measuring the ACF, the frequency is then measured. The key component in such systems is a photonic processing module (a dispersive element [7], [11], an optical mixing unit [9], [16], [17], or an optical filter [8], [10], [12]–[15], [18]–[20]) which provides two parallel channels with different, usually opposite, frequency-dependent power penalty functions. In most of the IFM schemes based on frequency-to-power mapping, an optical filter with a sinusoidal spectral response is employed to translate the frequency of the SUT to an optical power change. This would lead to an ACF with very poor linearity and the upper bound of unambiguous frequency measurement range is limited to the position of the first notch of the ACF. It is important for an IFM system to have a high and uniform measurement resolution and accuracy, thus a linear ACF is required to obtain an identical measurement sensitivity for the entire frequency measurement range. To achieve a linear ACF, a spe-

cial fiber Bragg grating (FBG) with two linear and complementary spectral slopes was employed to create two linear frequency-dependent power penalty functions [12]. A measurement range of 1-10 GHz with a uniform measurement accuracy of ±0.2 GHz was demonstrated [12]. An IFM system based on a silicon photonic integrated Fano Resonator was also proposed [20]. An R-squared value as large as 0.99 was obtained and the measurement range was 3-18 GHz with a resolution better than ±0.5 GHz [20]. Despite all these efforts, a common problem still severely limits the applications of the frequency-to-power mapping-based IFM methods: only single frequency signal can be measured. For many applications, multi-frequency measurement is needed.

For the techniques based on frequency-to-space mapping [21]–[24], the SUT is first modulated on an optical carrier, and then split into multiple space channels by an optical channelizer, to estimate its frequency at the outputs of the channelizer using a photodetector (PD) array. The key component in such systems is the optical channelizer which can be implemented by a Fabry-Perot etalon [21], [22], an arrayed-waveguide grating [23], or a diffraction grating [24]. The major problem associated with these techniques is the poor measurement resolution originated from the limited spectral resolution of an optical channelizer. In addition, the system is usually costly and complex due to the use of a large PD array.

For the techniques based on frequency-to-time mapping [25]–[28], the frequency of the SUT is converted into an electrical time delay using a dispersive time delay device [25] or a frequency shifting recirculating delay line (FS-RDL) [26], [27]. IFM with a uniform measurement resolution over the entire frequency measurement range can be achieved since a dispersive element has a linear group delay and a FS-RDL has equal frequency shift per roundtrip time. The key limitation of this approach is the limited measurement resolution. For example, the resolution of a dispersion-based method was as low as 12.5 GHz with a measurement error of about ±1.56 GHz [26]. In addition, the response time of the FS-RDL-based method is too long, which is not suitable for IFM. To improve the measurement resolution, an approach based on a Fourier domain mode-locked optoelectronic oscillator (FDML OEO) was proposed [28]. The frequency of the SUT is mapped to the time difference of the output pulses from the FDML OEO. The frequency measurement of single- and multi-frequency microwave signals was experimentally demonstrated with a measurement error of 60 MHz. However, limited by the bandwidth of the OEO, the frequency measurement range is only 15 GHz [28]. By using the time-space duality in a dispersive medium [i.e., a chirped FBG], a real-time Fourier transformation system for optical spectrum analysis was proposed [29]. Based on the same principle, a temporal pulse shaping system was reported to realize real-time electrical spectrum analysis [30]. Two dispersive elements (chirped FBGs) with complementary dispersion are connected before and after an MZM which is driven by a microwave SUT. The frequency information of the SUT is mapped to the time domain to have two temporal pulses with a time difference between the pulses corresponding to the frequency of the SUT [30]. Since the resolution is proportional to the dispersion amount of the chirped FBG, and a chirped FBG with an ultra-

high dispersion is usually difficult to fabricate, the resolution of this method is very limited. Moreover, the higher-order dispersion and miss-match between the two chirped FBGs will also affect the accuracy of the frequency measurement.

In this article, we propose and experimentally demonstrate a novel approach to achieve IFM based on frequency-to-time mapping using an FDML laser. When frequency-domain mode locking is achieved in the FDML laser, a linearly chirped optical waveform (LCOW) is generated [31]. Note that it is different from an LCOW generated by a frequency-tunable laser diode, in which the frequency is tuned with a longitudinal mode jumped to another longitudinal mode, but without phase locking. Thus, the phase noise is high. For an FDML laser, the longitudinal modes are phase locked, making the LCOW have low phase noise. The FDML laser is constructed by a long fiber ring cavity, with an erbium-doped fiber amplifier (EDFA) as a broadband gain medium and a tunable silicon microdisk resonator (MDR) as a narrow tunable optical bandpass filter (TOBPF). The SUT is modulated on an optical carrier at a dual-parallel Mach–Zehnder modulator (DP-MZM) to generate a single-sideband (SSB) signal with the help of an electrical 90° hybrid coupler. The SSB signal is combined with the light wave from the FDML laser and beat at a PD to generate an electrical chirped pulse train. The pulse train is then sent to a narrow bandpass filter (BPF) with a center frequency of f_{IF} to select the frequency component at f_{IF}. After envelope detection, a pair of short-duration temporal signals for each frequency component in the SSB signal is generated. Take the time delay of the optical carrier in the SSB signal as a reference, the frequency information of the SUT is mapped to the time difference between the corresponding short-duration temporal signals. A proof-of-concept experiment is carried out and single and multi-tone microwave frequency measurements are experimentally demonstrated. A frequency measurement resolution of 200 MHz and a measurement range as large as 20 GHz with an accuracy better than ±100 MHz is achieved.

II. PRINCIPLE

A. Fourier Domain Mode-Locked Laser

The key novelty of the proposed IFM approach is to use a Fourier domain mode-locked (FDML) laser as a broadband and linearly frequency-swept laser source, as shown in Fig. 1, for accurate frequency measurement. An FDML laser is different from a conventional frequency-swept laser which is usually implemented using a frequency-tunable BPF in the laser cavity, to sweep the lasing frequency. Since a laser needs a build-up time to stabilize the operation at a new frequency when the frequency-tunable BPF is tuned, the light generated by a conventional frequency-swept laser source has no fixed phase relationship for the frequencies within the pulse spectrum. For an FDML laser, however, the frequency-swept pulse is generated based on FDML, in which all longitudinal modes co-exist in the laser cavity with a fixed phase relationship. By tuning the TOBPF in the FDML laser cavity to select the longitudinal modes sequentially, a frequency swept optical pulse with fixed phase relationship for the frequencies within the pulse spectrum is generated. The TOBPF is driven by an electrical signal with its repetition period equal to the fundamental or 1/m of the cavity round-trip
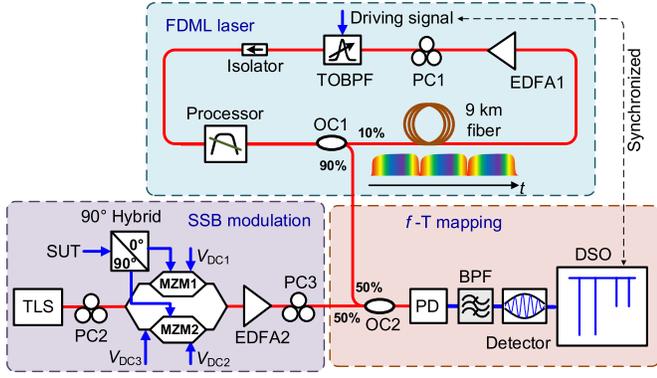
Fig. 1.   Schematic of the proposed IFM method based on frequency-to-time mapping using a FDML laser. SSB: single-sideband; SUT: signal under test; TLS: tunable laser source; PC: polarization controller; MZM: Mach–Zehnder modulator; EDFA: erbium-doped fiber amplifier; Processor: Finisar Waveshaper 4000S; OC: optical coupler; PD: photodetector; BPF: bandpass filter; DSO: digital storage oscilloscope; TOBPF: tunable optical bandpass filter.

time T_{cavity}, where m is an integer [31]. Note that the dispersion in the long fiber ring cavity is controlled to be zero to enable identical round-trip time for all longitudinal modes generated in the broadband gain medium. The dispersion management is achieved by the processor in Fig. 1. When these longitudinal modes pass sequentially through the TOBPF, frequency domain mode locking is achieved and a frequency-chirped pulse is generated. It should be noticed that the frequency distribution of an FDML pulse is determined by the driving function to the TOBPF. Applying a driving signal with a parabolic profile to the TOBPF, a LCOW is obtained [32]. Mathematically, the instantaneous frequency of a LCOW can be expressed as

$$f(t) = f_0 + \frac{B}{\tau}t, \quad -\tau/2 \le t \le \tau/2 \qquad (1)$$

where f_0, B, and τ are the center frequency, the bandwidth, and the duration of the pulse, respectively.

B. Single-Sideband With Carrier (SSB + C) Modulation

The SUT is modulated on an optical carrier at a DP-MZM to generate an SSB + C signal. The DP-MZM consists of two sub-MZMs embedded in a parent MZM, as shown in Fig. 1. To achieve SSB + C modulation, a continuous-wave (CW) optical carrier from a tunable laser source (TLS) is sent to the DP-MZM, to which the SUT is applied via an electrical 90° hybrid. By biasing the DP-MZM via tuning the three bias voltages, V_{DC1}, V_{DC2}, and V_{DC3}, an SSB + C signal is generated. A polarization controller (PC) is used before the DP-MZM to align the polarization direction of the optical carrier with the principal axis of the DP-MZM so that the polarization-dependent loss can be minimized.

The electrical field of the optical carrier from the TLS is given by

$$E_{\text{in}}(t) = E_0 e^{j\omega_c t} \qquad (2)$$

where E_0 is the electrical field amplitude and ω_c is the angular frequency of the optical carrier. Assuming electrical 90°
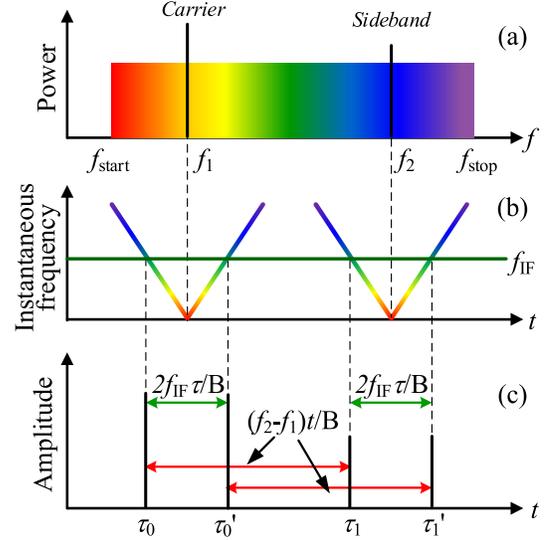
Fig. 2.   Principle of the proposed IFM system. (a) LCOW generated by the FDML laser and the generated SSB + C signal. (b) Instantaneous frequency of the beat signals between the LCOW and the SSB + C signal. (c) Two pairs of pulses after bandpass filtering. When the difference between the instantaneous frequency of the LCOW and that of the signal to be measured is equal to the center frequency of the BPF, a pair of short-duration temporal signals for each frequency component is generated and the time location represents the frequency of the signal to be measured.

hybrid has no insertion loss, and the microwave signals at the outputs of the 0° and 90° ports are $S_{e1} = V_e \cos(\omega_e t)$ and $S_{e2} = V_e \sin(\omega_e t)$, where V_e and ω_e are the amplitude and angular frequency of the microwave signals. Thus, the electrical field at the output of the DP-MZM can be expressed as

$$E_{\text{out}}(t) \propto e^{j\omega_c t}\left[E_{\text{MZM1}}(t) + E_{\text{MZM2}}(t)e^{j\varphi_3}\right]$$
$$\propto e^{j\omega_c t}\left[e^{j\beta\cos(\omega_e t)+j\varphi_1} + e^{j\beta\sin(\omega_e t)+j\varphi_2+j\varphi_3}\right] \qquad (3)$$

where $E_{\text{MZM1}}(t)$ and $E_{\text{MZM2}}(t)$ are the electrical fields at the outputs of the upper and lower sub-MZMs, respectively, $\varphi_3 = \pi V_{\text{DC3}}/V_\pi'$ is the phase shift between the sub-MZMs, V_π' is the microwave half-wave voltage of the parent MZM, $\beta = \pi V_e/V_\pi$ is the modulation index, V_π is the microwave half-wave voltage of the sub-MZMs, and $\varphi_i = \pi V_{\text{DC}i}/V_\pi$ ($i = 1, 2$) are the bias angles of the upper and lower sub-MZMs, respectively. Using Jacobi–anger expansion, (3) can be further expressed as

$$E_{\text{out}}(t) \propto e^{j\omega_c t}\left[e^{j\varphi_1}\sum_{n=-\infty}^{\infty}j^n J_n(\beta)e^{jn\omega_e t}\right.$$
$$\left. + e^{j\varphi_2+j\varphi_3}\sum_{n=-\infty}^{\infty}j^n J_n(\beta)e^{jn(\omega_e t-\pi/2)}\right] \qquad (4)$$

where $J_n(\beta)$ is the nth-order Bessel functions of the first kind. Ignoring the higher-order sidebands and the intermodulation terms (≥ 2) and adjusting the bias voltages to make $\varphi_1 = \varphi_2 = \varphi_3 = \pi/2$, the optical field at the output of the DP-MZM is given by

$$E_{\text{out}}(t) \propto e^{j\omega_c t}\left[(j-1)J_0(\beta) - 2J_1(\beta)e^{j\omega_e t}\right]. \qquad (5)$$

As can be seen from (5), only the optical carrier and one first-order optical sideband (+1st order) exist, thus an SSB + C modulation is achieved.

C. Photonic IFM Based on Frequency-to-Time Mapping

The generated SSB + C signal is combined with the light wave from the FDML laser and sent to a PD where a beat signal is generated. Note that the chirped pulse generated by the FDML laser has a locked phase, as shown in Fig. 2(a). The IFM is realized based on frequency-to-time mapping, to translate the frequency information to a time delay, with the principle shown in Fig. 2. As can be seen, after beating between an LCOW from the FDML laser with a CW optical signal, the frequency of the FDML pulse is down-converted to the microwave band. As shown in Fig. 2(b), when the instantaneous frequency of the FDML pulse is lower (or higher) than the frequency of the SSB + C signal, after beating at the PD two linearly frequency modulated (LFM) signals with a chirp rate of $-B/\tau$ (or B/τ) is generated. If a BPF with a center frequency at f_{IF} and a 3-dB bandwidth of BW is connected to the PD, two pairs of short pulses with a time difference between the two pulses in a pair being $2f_{IF}\tau/B$ is generated, as shown in Fig. 2(c). The center point between a pulse pair corresponds to the zero instantaneous frequency of a beat signal, which indicates that the frequency of the SSB or the carrier signal is equal to the instantaneous frequency of the FDML pulse at that particular time. If a narrowband lowpass filter (LPF) is applied, $f_{IF} = 0$, only a single pulse (instead of a pair of pulses) is generated and its temporal location corresponds to the zero instantaneous frequency of a beat signal. In comparison, the use of a BPF can slightly reduce the measurement error since the center point is the average of the two time measurements rather than a single time measurement. In addition, a BPF can usually have a narrower bandwidth, which would make the frequency measurement more accurate. In our implementation, a BPF rather than an LPF is used.

At the output of the BPF, for a single-frequency input, a pair of pulses with a time delay difference between the two pulses being $2f_{IF}\tau/B$ is then obtained. For an SSB + C signal, two pairs of pulses representing the beating between the optical carrier and the sideband with the LCOW, as shown in Fig. 2(c). By monitoring the time delays at the pulses, the frequency of the SUT can be estimated, which is given by

$$f_e = f_2 - f_1 = \frac{B}{\tau}(\tau_1 - \tau_0) = \frac{B}{\tau}(\tau_1' - \tau_0') \qquad (6)$$

where f_1, f_2 are the frequency of the optical carrier and the first-order sideband, respectively; τ_0, τ_1, are the time delays of the pulses resulting from the optical carrier, and τ_0' and τ_1' are the time delays of the pulses resulting from the first-order sideband. The theoretical 3-dB temporal width of the short pulses is determined by the rise-and-fall time ($2 \times 0.35/$BW) of the filter [33]. Thus, the theoretical frequency measurement resolution can be calculated based on the frequency-to-time mapping relationship, given by

$$r = \frac{0.7B}{\tau \cdot \text{BW}} \qquad (7)$$

where B/τ is the chirp rate of the LCOW.

III. EXPERIMENTAL DEMONSTRATION

A proof-of-concept experiment based on the setup in Fig. 1 is carried out. The key device in the system is the FDML laser,
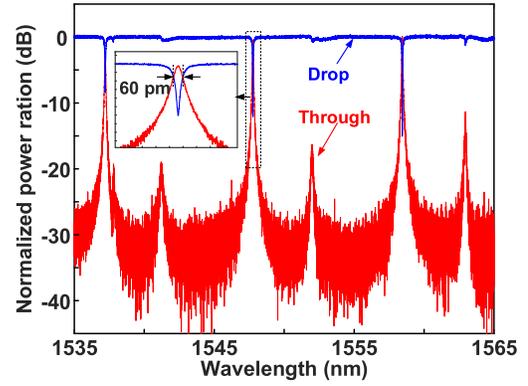
Fig. 3. Transmission response of the MDR.

which is implemented with a fiber ring geometry incorporating an EDFA (Nortel) as a broadband gain medium. A PC is inserted between the EDFA and the TOBPF to minimize the polarization-dependent cavity loss. The TOBPF is a tunable silicon MDR which has a relatively narrow passband and can be fast tunable. The spectral responses of the MDR at the drop and through ports are measured by an optical vector analyzer (LUNA OVA CTe) and shown in Fig. 3. As can be seen from the zoomed-in view in Fig. 3, a 3-dB bandwidth of 60 pm (~7.5 GHz @ 1550 nm) is obtained. The MDR is driven by a periodic parabolic signal generated by an arbitrary waveform generator (AWG, Agilent 33250A) with a repetition rate of 23.39 kHz, corresponding to the round-trip time of the ring cavity. An isolator is used to form a unidirectional anticlockwise propagation of the longitudinal modes. Since the gain bandwidth of the EDFA covers two times the free spectral range (FSR) of the MDR, an optical processor (Finisar Waveshaper 4000S) is used to select the resonance around 1550 nm. The optical processor is also used as a device for dispersion compensation to manage the dispersion in the cavity. An optical coupler (OC1) is used to split the optical signal into two parts, with 10% of the optical power fed back via a 9 km non-zero dispersion-shifted fiber (NZDSF) to close the FDML laser loop while 90% of the optical power being combined with the SSB + C signal and applied to the PD. The spectrum of the light generated by the FDML is shown in Fig. 4(a) and the instantaneous frequency of the beat signal with a CW light is shown in Fig. 4(b). The chirp rate of the LCOW in our experiment is 2.74 GHz/μs. The bandwidth of the FDML laser is about 0.5 nm (~62.5 GHz @ 1550 nm), which is wide enough for IFM application. The spectrogram of the beat signal shows that the FDML laser has good frequency linearity, which is required to keep a uniform measurement resolution and accuracy within the measurement range.

An optical carrier from a TLS (Anritsu MG9638A) emitting at 1548.5 nm with a power of 8 dBm is generated, which is sent to the DP-MZM via the electrical 90° hybrid coupler where it is modulated by a microwave signal from a microwave source (Agilent E8254A). The DP-MZM (JDS Uniphase, Model 470661H) has a bandwidth of 20 GHz. The bias voltages applied to the upper sub-MZM, lower sub-MZM, and parent MZM are 5.06 V (V_{DC1}), 4.79 V (V_{DC2}), and 7.59 V (V_{DC3}), respectively. Fig. 5 shows the spectrum of the
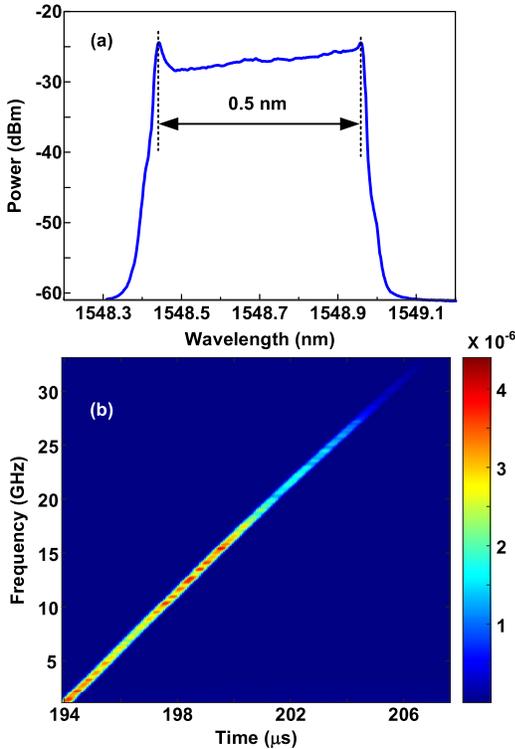
Fig. 4. (a) Optical spectrum of the LCOW generated by the FDML laser. (b) Instantaneous frequency of the beat signal with a CW laser.
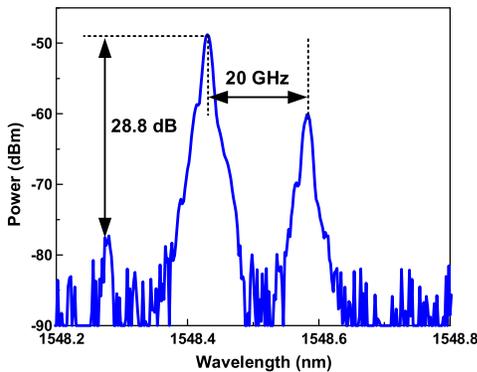
Fig. 5. Spectrum of the SSB + C signal.

Fig. 6. Frequency response of the electrical bandpass filter.
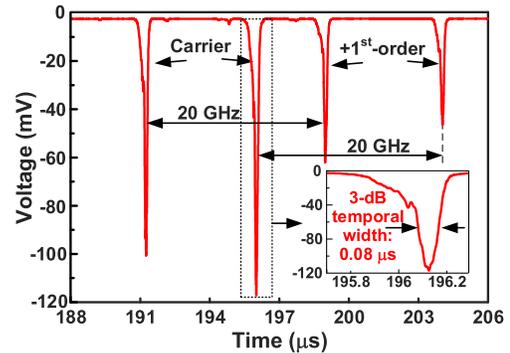
Fig. 7. Temporal waveform recorded by the DSO when the frequency of an input microwave signal is 20 GHz.
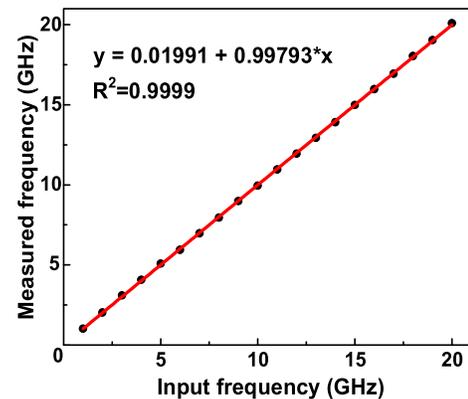
Fig. 8. Measured frequency versus the input frequency when the electrical power level of the input signal is at 19 dBm.

SSB + C signal when the microwave signal at 20 GHz is applied. A sideband suppression ratio as high as 28.8 dB is achieved. The SSB + C signal is amplified and combined with the light from the FDML laser to beat at a 10 GHz PD (Lucent Model 2623CSA). The beat signal is then sent to a BPF centered at 6.19 GHz before envelope detection (Detector, 0.1-20 GHz, Model 201S). The frequency response of the BPF is shown in Fig. 6. As can be seen, the 3-dB bandwidth of the BPF is 30 MHz and the rise-and-fall time of the BPF is 0.023 μs. Thus, the theoretical frequency measurement resolution is calculated to be 63 MHz. A BPF with a narrower bandwidth would lead to a better accuracy. The temporal waveform recorded by the digital storage oscilloscope (DSO) (sampling rate 1 GSa/s, Agilent DSO-X 93204A) when the input microwave signal is 20 GHz is shown in Fig. 7. The 3-dB temporal width of the short pulses is about 0.08 μs, thus the

frequency measurement resolution of the proposed system is about 200 MHz. The resolution deterioration mainly originates from the poor wavelength stability of the TLS and the LCOW, and the interpolation error of the DSO.

Two pairs of notches are observed. Note that the envelope detector gives an inverted output, making two notches corresponding to the two shown in Fig. 2(c). Fig. 8 shows the measured frequency versus the input frequency when the power level of the input electrical signal is at 19 dBm. An R-square value as high as 0.9999 is achieved. Without electrical power amplification or attenuation to the SUT, a dynamic range of 29 dB is achieved. The measurement
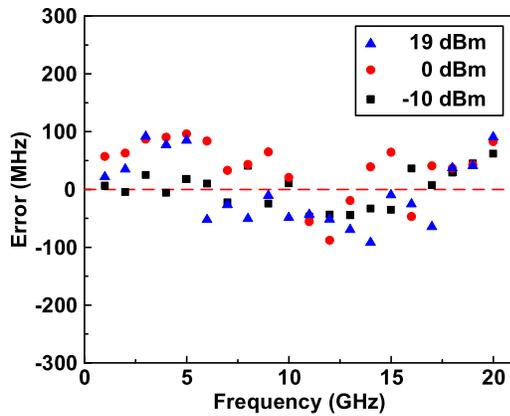
Fig. 9. Measurement errors when the electrical power levels of the input signals are 19, 0, and −10 dBm, respectively.

Fig. 10. Frequency measurement resolution.

Fig. 11. (a) Electrical spectrum of the 3-tone RF signal. (b) Temporal waveform of the 3-tone RF signal input. (c) Frequency measurement errors.

errors are also measured, which are shown in Fig. 9 when the power levels of the input signals are at 19, 0, and −10 dBm. For a measurement range of 20 GHz, an accuracy better than ±100 MHz is achieved. Then measurement resolution of 200 MHz is shown in Fig. 10 when the SUT is a two-tone microwave signal (18 and 18.2 GHz). To verify the feasibility of multi-frequency measurement, a 3-tone microwave signal is generated by another AWG (Keysight M8195A) as the SUT. The electrical spectrum of the 3-tone microwave signal is shown in Fig. 11(a) and temporal waveform recorded by the DSO is shown in Fig. 11(b). Then the measurement error for each tone is calculated and shown in Fig. 11(c).

It should be noted that the measurement updating rate is at the order of the driving frequency of the MDR (23.39 kHz), indicating that a very fast frequency measurement is achieved. In addition, as compared with the method based on an FDML OEO [28], the proposed IFM system has a much wider frequency measurement range. The DP-MZM is the only high-speed device needed in this system and the bandwidth of which limits the upper bound of the measurement range. If an optical modulator with a wider modulation bandwidth (for instance a plasmonic-based modulator) is employed, the measurement range of the proposed IFM system could be expanded to even sub-THz while maintaining the same measurement accuracy and speed. Moreover, the measurement accuracy of the proposed method is mainly affected by the

wavelength stability of the TLS and the 3-dB bandwidth of the BPF. If a more stable TLS and a narrower bandwidth BPF are employed, the measurement resolution could be comparable or even better than that reported in [28].

IV. CONCLUSION

A novel approach to broadband instantaneous multi-frequency measurement using an FDML laser was proposed and experimentally demonstrated. The key device in the measurement system is an electrically controlled silicon MDR with a linewidth of 60 pm (∼7.5 GHz) inserted in the FDML loop to realize a high-speed and ultra-narrow optical filtering, leading to effective frequency-domain mode locking. By using the output from the FDML laser which was a broadband frequency-swept chirped pulse and beating it with an SSB + C signal at a low-speed PD, the frequency information of the SUT was mapped to the time domain. By monitoring the time delays using a low-speed oscilloscope, the frequency of the SUT could be measured. One key advantage of the approach is that it can measure multiple frequencies at a high speed. The approach was experimentally evaluated. In our proof-of-concept experiment, a measurement range as large as 20 GHz with a measurement resolution of 200 MHz and an accuracy better than ±100 MHz was achieved. The measurement range can be extended if a wider bandwidth DP-MZM is used. The approach has potential applications in the radar, electronic warfare, communications, and cognitive radio systems.

REFERENCES

[1] R. G. Wiley, *Electronic Intelligence: The Analysis of Radar Signals*. Boston, MA, USA: Artech House, 1993.

[2] A. E. Spezio, "Electronic warfare systems," *IEEE Trans. Microw. Theory Techn.*, vol. 50, no. 3, pp. 633–644, Mar. 2002.

[3] P. W. East, "Fifty years of instantaneous frequency measurement," *IET Radar, Sonar Navigat.*, vol. 6, no. 2, pp. 112–122, Feb. 2012.

[4] J. Yao, "Microwave photonics," *J. Lightw. Technol.*, vol. 27, no. 3, pp. 314–335, Feb. 1, 2009.

[5] X. Zou, B. Lu, W. Pan, L. Yan, A. Stöhr, and J. Yao, "Photonics for microwave measurements," *Laser Photon. Rev.*, vol. 10, no. 5, pp. 711–734, Jul. 2016.

[6] S. L. Pan and J. Yao, "Photonics-based broadband microwave measurement," *J. Lightw. Technol.*, vol. 35, no. 16, pp. 3498–3513, Aug. 15, 2017.

[7] L. V. T. Nguyen and D. B. Hunter, "A photonic technique for microwave frequency measurement," *IEEE Photon. Technol. Lett.*, vol. 18, no. 10, pp. 1188–1190, May 15, 2006.

[8] H. Chi, X. Zou, and J. Yao, "An approach to the measurement of microwave frequency based on optical power monitoring," *IEEE Photon. Technol. Lett.*, vol. 20, no. 14, pp. 1249–1251, Jul. 15, 2008.

[9] M. Pelusi *et al.*, "Photonic-chip-based radio-frequency spectrum analyser with terahertz bandwidth," *Nature Photon.*, vol. 3, pp. 139–143, Feb. 2009.

[10] X. Zou, H. Chi, and J. Yao, "Microwave frequency measurement based on optical power monitoring using a complementary optical filter pair," *IEEE Trans. Microw. Theory Techn.*, vol. 57, no. 2, pp. 505–511, Feb. 2009.

[11] X. Zou, S. Pan, and J. Yao, "Instantaneous microwave frequency measurement with improved measurement range and resolution based on simultaneous phase modulation and intensity modulation," *J. Lightw. Technol.*, vol. 27, no. 23, pp. 5314–5320, Dec. 1, 2009.

[12] Z. Li, C. Wang, M. Li, H. Chi, X. Zhang, and J. Yao, "Instantaneous microwave frequency measurement using a special fiber Bragg grating," *IEEE Microw. Wireless Compon. Lett.*, vol. 21, no. 1, pp. 52–54, Jan. 2011.

[13] S. Pan, J. Fu, and J. Yao, "Photonic approach to the simultaneous measurement of the frequency, amplitude, pulse width, and time of arrival of a microwave signal," *Opt. Lett.*, vol. 37, no. 1, pp. 7–9, 2012.

[14] D. Marpaung, "On-chip photonic-assisted instantaneous microwave frequency measurement system," *IEEE Photon. Technol. Lett.*, vol. 25, no. 9, pp. 837–840, May 1, 2013.

[15] J. S. Fandiño and P. Muñoz, "Photonics-based microwave frequency measurement using a double-sideband suppressed-carrier modulation and an InP integrated ring-assisted Mach–Zehnder interferometer filter," *Opt. Lett.*, vol. 38, no. 21, pp. 4316–4319, Nov. 2013.

[16] H. Emami and M. Ashourian, "Improved dynamic range microwave photonic instantaneous frequency measurement based on four-wave mixing," *IEEE Trans. Microw. Theory Techn.*, vol. 62, no. 10, pp. 2462–2470, Oct. 2014.

[17] M. Pagani *et al.*, "Low-error and broadband microwave frequency measurement in a silicon chip," *Optica*, vol. 2, no. 8, pp. 751–756, Aug. 2015.

[18] H. Jiang *et al.*, "Wide-range, high-precision multiple microwave frequency measurement using a chip-based photonic Brillouin filter," *Optica*, vol. 3, no. 1, pp. 30–34, Jan. 2016.

[19] M. Burla, X. Wang, M. Li, L. Chrostowski, and J. Azaña, "Wideband dynamic microwave frequency identification system using a low-power ultracompact silicon photonic chip," *Nature Commun.*, vol. 7, p. 13004, Sep. 2016.

[20] B. Zhu, W. Zhang, S. Pan, and J. Yao, "High-sensitivity instantaneous microwave frequency measurement based on a silicon photonic integrated Fano resonator," *J. Lightw. Technol.*, vol. 37, no. 11, pp. 2527–2533, Jun. 1, 2019.

[21] S. T. Winnall, A. C. Lindsay, M. W. Austin, J. Canning, and A. Mitchell, "A microwave channelizer and spectroscope based on an integrated optical Bragg-grating Fabry–Perot and integrated hybrid Fresnel lens system," *IEEE Trans. Microw. Theory Techn.*, vol. 54, no. 2, pp. 868–872, Feb. 2006.

[22] L. X. Wang, N. H. Zhu, W. Li, H. Wang, J. Y. Zheng, and J. G. Liu, "Polarization division multiplexed photonic radio-frequency channelizer using an optical comb," *Opt. Commun.*, vol. 286, pp. 282–287, Jan. 2013.

[23] J. M. Heaton *et al.*, "16-channel (1-to 16-GHz) microwave spectrum analyzer device based on a phased array of GaAs/AlGaAs electro-optic waveguide delay lines," *Proc. SPIE*, vol. 3278, pp. 245–251, Jan. 1998.

[24] X. Zou, W. Li, W. Pan, L. Yan, and J. Yao, "Photonic-assisted microwave channelizer with improved channel characteristics based on spectrum-controlled stimulated Brillouin scattering," *IEEE Trans. Microw. Theory Techn.*, vol. 61, no. 9, pp. 3470–3478, Sep. 2013.

[25] L. V. T. Nguyen, "Microwave photonic technique for frequency measurement of simultaneous signals," *IEEE Photon. Technol. Lett.*, vol. 21, no. 10, pp. 642–644, May 15, 2009.

[26] T. A. Nguyen, E. H. W. Chan, and R. A. Minasian, "Instantaneous high resolution multiple-frequency measurement system based on frequency-to-time mapping technique," *Opt. Lett.*, vol. 39, no. 8, pp. 2419–2422, Apr. 2014.

[27] T. A. Nguyen, E. H. W. Chan, and R. A. Minasian, "Photonic multiple frequency measurement using a frequency shifting recirculating delay line structure," *J. Lightw. Technol.*, vol. 32, no. 20, pp. 3831–3838, Oct. 15, 2014.

[28] T. Hao, J. Tang, W. Li, N. Zhu, and M. Li, "Microwave photonics frequency-to-time mapping based on a Fourier domain mode locked optoelectronic oscillator," *Opt. Exp.*, vol. 26, no. 26, pp. 33582–33591, Dec. 2018.

[29] J. Azana and M. A. Muriel, "Real-time optical spectrum analysis based on the time-space duality in chirped fiber gratings," *IEEE J. Quantum Electron.*, vol. 36, no. 5, pp. 517–526, May 2000.

[30] J. Azana, N. K. Berger, B. Levit, and B. Fischer, "Reconfigurable generation of high-repetition-rate optical pulse sequences by time-domain phase-only filtering," *Opt. Lett.*, vol. 30, no. 23, pp. 3228–3230, Dec. 2005.

[31] R. Huber, M. Wojtkowski, and J. G. Fujimoto, "Fourier domain mode locking (FDML): A new laser operating regime and applications for optical coherence tomography," *Opt. Exp.*, vol. 14, no. 8, pp. 3225–3237, 2006.

[32] J. Tang, B. Zhu, W. Zhang, M. Li, S. Pan, and J. Yao, "Hybrid Fourier-domain mode-locked laser for ultra-wideband linearly chirped microwave waveform generation," *Nature Commun.*, vol. 11, no. 1, Jul. 2020, Art. no. 3814.

[33] C. Mittermayer and A. Steininger, "On the determination of dynamic errors for rise time measurement with an oscilloscope," *IEEE Trans. Instrum. Meas.*, vol. 48, no. 6, pp. 1103–1107, Dec. 1999.

Beibei Zhu received the B.S. degree from Nanjing University of Aeronautics and Astronautics, Nanjing, China, in 2013, where she is currently pursuing the Ph.D. degree at the Key Laboratory of Radar Imaging and Microwave Photonics, Ministry of Education.

She was a Visiting Student with the Microwave Photonics Research Laboratory, School of Electrical Engineering and Computer Science, University of Ottawa, Ottawa, ON, Canada, from September 2017 to March 2019. Her current research interests include microwave photonic measurement techniques and applications.

Jian Tang received the B.Sc. degree in material physics from the University of Science and Technology of China, Hefei, China, in 2013, and the Ph.D. degree in integrated microwave photonics from the Institute of Semiconductors, CAS, Beijing, China, in 2019.

From 2017 to 2019, he joined the Microwave Photonics Research Laboratory, School of Electrical Engineering and Computer Science, University of Ottawa, Ottawa, ON, Canada, as a joint-training Ph.D. Student. His research interests include the integrated microwave photonics signal processing and optical communication.

Weifeng Zhang (Member, IEEE) received the B.Eng. degree in electronic science and technology from Xi'an Jiaotong University, Xi'an, China, in 2008, the M.A.Sc. degree in electrical engineering from the Politecnico di Torino, Turin, Italy, in 2011, and the Ph.D. degree in electrical engineering from the University of Ottawa, Ottawa, ON, Canada, in 2017.

From June 2017 to May 2019, he was a Post-Doctoral Fellow with the University of Ottawa. In June 2019, he joined the School of Information and Electronics, Beijing Institute of Technology, Beijing, China, as a Full Professor. His current research interests include silicon photonics and integrated microwave photonics.

Shilong Pan (Senior Member, IEEE) received the B.S. and Ph.D. degrees in electronics engineering from Tsinghua University, Beijing, China, in 2004 and 2008, respectively.

From 2008 to 2010, he was a "Vision 2010" Post-Doctoral Research Fellow with the Microwave Photonics Research Laboratory, University of Ottawa, Ottawa, ON, Canada. He joined the College of Electronic and Information Engineering, Nanjing University of Aeronautics and Astronautics, Nanjing, China, in 2010, where he is currently a Full Professor and an Executive Director of the Key Laboratory of Radar Imaging and Microwave Photonics, Ministry of Education. He has authored or coauthored over 380 research papers, including more than 200 articles in peer-reviewed journals and 180 papers in conference proceedings. His research interests include microwave photonics, which includes optical generation and processing of microwave signals, analog photonic links, photonic microwave measurement, and integrated microwave photonics.

Prof. Pan is also a Fellow of the Optical Society (OSA), International Society for Optical Engineering (SPIE), and Institution of Engineering and Technology (IET). He was selected to receive an OSA Outstanding Reviewer Award in 2015 and a Top Reviewer of IEEE/OSA JOURNAL OF LIGHTWAVE TECHNOLOGY in 2016. He was awarded the Excellent Young Scholars Award of the National Natural Science Foundation of China in 2014, and the Scientific and Technological Innovation Leading Talents Award of the National Ten Thousand Plan in 2018. He was selected as an IEEE Photonics Society Distinguished Lecturer in 2019.

Jianping Yao (Fellow, IEEE) received the Ph.D. degree in electrical engineering from the Université de Toulon, Toulon, France, in December 1997.

From 1998 to 2001, he was an Assistant Professor with the School of Electrical and Electronic Engineering, Nanyang Technological University (NTU), Singapore. In December 2001, he joined the School of Electrical Engineering and Computer Science, University of Ottawa, Ottawa, ON, Canada, as an Assistant Professor, where he was promoted to an Associate Professor in May 2003, and a Full Professor in May 2006. He was appointed as the University Research Chair of microwave photonics in 2007. In June 2016, he was conferred the title of Distinguished University Professor of the University of Ottawa. From July 2007 to June 2010 and from July 2013 to June 2016, he was the Director of the Ottawa-Carleton Institute for Electrical and Computer Engineering, Ottawa, ON, Canada. He is currently a Distinguished University Professor and the University Research Chair with the School of Electrical Engineering and Computer Science, University of Ottawa. He has authored or coauthored over 620 research papers including over 360 articles in peer-reviewed journals and over 260 papers in conference proceedings.

Prof. Yao has served as a Committee Member for a number of international conferences, such as the IEEE Photonics Conference (IPC), Optical Fiber Communication Conference and Exposition (OFC), Bragg Gratings, Photosensitivity, and Poling in Glass Waveguides (BGPP), and International Topical Meeting on Microwave Photonics (MWP). He was a member of the European Research Council Consolidator Grant Panel in 2016, 2018, and 2020, the Qualitative Evaluation Panel in 2017, and a panelist of the National Science Foundation Career Awards Panel in 2016. He was an Elected Member of the Board of Governors of the IEEE Photonics Society from 2019 to 2021. He is also a Fellow of the Optical Society of America, the Canadian Academy of Engineering, and the Royal Society of Canada. He received the 2005 International Creative Research Award of the University of Ottawa. He was a recipient of the 2007 George S. Glinski Award for Excellence in Research. In 2008, he was awarded the Natural Sciences and Engineering Research Council of Canada Discovery Accelerator Supplements Award. He was selected to receive an Inaugural OSA Outstanding Reviewer Award in 2012. He was one of the top ten reviewers of IEEE/OSA JOURNAL OF LIGHTWAVE TECHNOLOGY from 2015 to 2016. He also received the 2017-2018 Award for Excellence in Research of the University of Ottawa. He was also a recipient of the 2018 R.A. Fessenden Silver Medal from IEEE Canada. He also serves as the Technical Committee Chair for IEEE MTT-S Microwave Photonics. He has also served as the Chair of a number of international conferences, symposia, and workshops, including the Vice Technical Program Committee (TPC) Chair of the 2007 IEEE Topical Meeting on Microwave Photonics, the TPC Co-Chair of the 2009 and 2010 Asia-Pacific Microwave Photonics Conference, the TPC Chair of the High-Speed and Broadband Wireless Technologies Subcommittee of the IEEE Radio Wireless Symposium 2009–2012, the Microwave Photonics Subcommittee of the IEEE Photonics Society Annual Meeting 2009, and the 2010 IEEE Topical Meeting on Microwave Photonics, the General Co-Chair of the 2011 IEEE Topical Meeting on Microwave Photonics, the TPC Co-Chair of the 2014 IEEE Topical Meetings on Microwave Photonics, the General Co-Chair of the 2015 and 2017 IEEE Topical Meeting on Microwave Photonics, and the General Chair of the 2019 IEEE Topical Meeting on Microwave Photonics. He was an IEEE MTT-S Distinguished Microwave Lecturer from 2013 to 2015. He is also a registered Professional Engineer of Ontario. He is also the Editor-in-Chief of IEEE PHOTONICS TECHNOLOGY LETTERS, a Former Topical Editor of *Optics Letters*, a Former Associate Editor of Science Bulletin, a Steering Committee Member of IEEE JOURNAL OF LIGHTWAVE TECHNOLOGY, and an Advisory Editorial Board Member of *Optics Communications*. He was a Guest Editor of a Focus Issue on Microwave Photonics in Optics Express in 2013, a Lead-Editor of a Feature Issue on Microwave Photonics in Photonics Research in 2014, and a Guest Editor of a Special Issue on Microwave Photonics in IEEE/OSA JOURNAL OF LIGHTWAVE TECHNOLOGY in 2018.